Full-field refractive index measurement with simultaneous phase-shift interferometry

Yen-Chang Chu [a], Wei-Yao Chang [b], Kun-Huang Chen [c,*], Jing-Heng Chen [d], Bo-Chung Tsai [c], Ken Y. Hsu [b]

[a] Ph.D. program of Electrical and Communications Engineering, Feng Chia University, No.100, Wen Hwa Rd., Taichung 40724, Taiwan, ROC
[b] Department of Photonics and Institute of Electro-Optical Engineering, National Chiao Tung University, 1001 Ta-Hsueh Road, Hsinchu 30050, Taiwan, ROC
[c] Department of Electrical Engineering, Feng Chia University, No.100, Wen Hwa Rd., Taichung 40724, Taiwan, ROC
[d] Department of Photonics, Feng Chia University, No.100, Wen Hwa Rd., Taichung 40724, Taiwan, ROC

ARTICLE INFO

ABSTRACT

Using the phenomenon of total internal reflection and a beam splitting device, a technique of simultaneous phase-shift interferometry is proposed for measuring the full-field refractive index. Because this method applies a beam splitting device that mimics the characteristics of beam splitting and phase modulation, four interferemetric images of various phase distributions can be simultaneously captured. Therefore, this setup can avoid errors caused by non-simultaneous capturing of images and offers the benefits of high stability, ease of operation, and real-time measurement. Furthermore, using the phenomenon of total internal reflection, the phase difference between p- and s-polarized light varies considerably with the refractive index of a tested specimen. This can substantially increase the measurement resolution. The feasibility of this method is verified using an experiment, and the measurement resolution can be higher than 3.65×10^{-4} RIU.
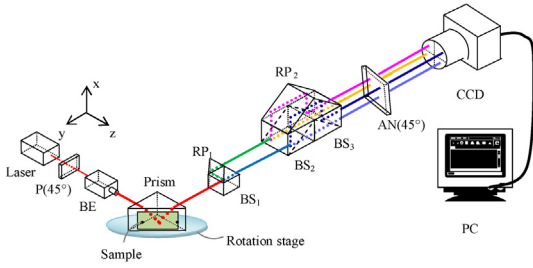
1. Introduction

The measurement of the full-field refractive index plays a crucial role in numerous research and industrial fields, such as the inspection of optical components [1], characteristic measurements of thin-films [2], biology, and medicine [3], [4]. Interferometry is an accurate method for measuring the refractive index [5]. The phase difference between the tested beam and the reference beam in an interferometer can be used to estimate the refractive index of the sample. The phase-shifting method is an effective technique for extracting the phase difference. Traditional phase-shifting methods introduce successive phase steps into interferometric signals by using various phase-shifting strategies, such as PZT [6], [7], EOM [8], and SLM [9], [10]. The traditional phase-shifting interferometric methods feature simple structures and easy operation. However, they are time consuming because they repeatedly capture images and the measuring results are easily affected by the disturbance of the surrounding environment. Synchronous phase-shift methods use novel techniques or components to obtain the successive phase-shifting signals in one shot [11]. Although the synchronous

phase-shift methods have the advantages of high measurement sensitivity and real-time image capture, they have complicated structures and high cost. Therefore, this paper presents a technique of simultaneous phase-shift interferometry for the measurement of the full-field refractive index. This technique applies the phenomenon of total internal reflection of a collimated beam on the interface of a prism and tested specimens. Substantial phase variations, which are a refractive-index function of the measurement samples, can be introduced into the reflection fields. Four interferometric images of various phase distributions can be simultaneously obtained by applying a beam splitting device. Finally, these images are captured by a CCD camera and full-field refractive-indices can be determined using specifically derived equations. Various mixtures of the tested specimens were measured during the experiments. The measured results corresponded with the theoretical values. The measurement resolution can be higher than 3.65×10^{-4} RIU. This method has the advantages of a simple structure, high stability, ease of operation, and real-time measurement.

2. Principle

Fig. 1 shows the experimental setup for this measurement. For convenience, the +z-axis was set as the direction of light propagation and the y-axis projects perpendicularly to the plane of the

* Corresponding author. Tel.: +886 4 2451 7250x3831; fax: +886 4 2451 6842.
 E-mail address: chenkh@fcu.edu.tw (K.-H. Chen).

Fig. 1. Optical configuration of full-field refractive index measurement. P: polarizer; BE: beam expander; BS: beam splitter; RP: right-angle prism; AN: analyzer; CCD: CMOS camera; PC: personal computer.

paper. A linear polarized laser light with a polarization state of 45° relative to the x-axis was expanded and collimated using a beam expander (BE) to form a plane wave. The plane wave was incident at θ_1 onto the boundary surface between a right-angle prism and a tested specimen. The total internal refraction (TIR) appeared when the incident angle was larger than the critical angle, $\theta_c = \sin^{-1}(n_2/n_1)$, where parameters n_1 and n_2 are the refractive indices of the prism and the tested specimen, respectively. The reflected light was incident on a beam splitting device, and was divided into two parts by beam splitter BS_1: the transmitted light, and the reflected light. The transmitted light was incident on BS_2, and was divided into a further two parts: transmitted and reflected lights. The paths of these two beams are $RP_2 \rightarrow BS_3 \rightarrow AN \rightarrow CCD$ (to generated test signal I_1) and $BS_3 \rightarrow AN \rightarrow CCD$ (to generated test signal I_2). When the transmission axis of AN was set 45° to the x-axis, the detected intensities of I_1 and I_2 were

$$I_1 = I_0[1 + \gamma \cos(\phi + 2\phi_{BS} + 2\phi_{RP})], \qquad (1)$$

and

$$I_2 = I_0[1 + \gamma \cos(\phi)], \qquad (2)$$

where I_0 and γ are the bias intensity and the visibility of the signal, respectively, and ϕ is the phase difference between the p- and s-polarized light from the reflection at the boundary surface under the conditions of TIR. These terms are expressed as

$$I_0 = \frac{|r_p|^2 + |r_s|^2}{4}, \qquad (3a)$$

$$\gamma(x,y) = \frac{2|r_p||r_s|}{|r_p|^2 + |r_s|^2}, \qquad (3b)$$

$$\phi = \phi_p - \phi_s = \arg(r_p) - \arg(r_s), \qquad (3c)$$

where ϕ_p and ϕ_s are the phase retardations of the p- and s-polarized light, and r_p and r_s are the reflection coefficients of the p- and s-polarized light, respectively. These parameters can be written as

$$r_p = \frac{n^2 \cos\theta_1 - i\sqrt{\sin^2\theta_1 - n^2}}{n^2 \cos\theta_1 + i\sqrt{\sin^2\theta_1 - n^2}} = |r_p| e^{i\phi_p}, \qquad (4)$$

$$r_s = \frac{\cos\theta_1 - i\sqrt{\sin^2\theta_1 - n^2}}{\cos\theta_1 + i\sqrt{\sin^2\theta_1 - n^2}} = |r_s| e^{i\phi_s}, \qquad (5)$$

where $n = n_2/n_1$ is the relative refractive index. In addition, ϕ_{BS} and ϕ_{RP} denote the phase differences between the p- and s-polarizations produced by the reflections at the BS and prism, respectively. By substituting Eqs. (4) and (5) into Eq. (3c), the

relationship of the relative refractive index n and the incident angle θ_1 can be expressed as

$$\phi(n, \theta_1) = -2\tan^{-1}\left(\frac{\sqrt{\sin^2\theta_1 - n^2}}{\tan\theta_1 \sin\theta_1}\right). \qquad (6)$$

Eq. (6) can be rewritten as:

$$n_2 = n_1 \sin(\theta_1)\left[1 - \tan^2\left(\frac{\phi}{2}\right) \cdot \tan^2(\theta_1)\right]^{1/2}. \qquad (7)$$

According to Eq. (7), the refractive index n_2 of the tested specimen is the function of the phase difference ϕ.

On the other hand, the reflected light from BS_1 was reflected again by a right-angle prism RP_1. The reflected light was incident on BS_2, and was divided into two parts: transmitted and reflected lights. The paths of these two beams are $RP_2 \rightarrow BS_3 \rightarrow AN \rightarrow CCD$ (to generated test signal I_3) and $BS_3 \rightarrow AN \rightarrow CCD$ (to generated test signal I_4). When the transmission axis of AN was set 45° to the x-axis, the detected intensities of I_3 and I_4 were

$$I_3 = I_0(1 + \gamma \cos(\phi + 3\phi_{BS} + 3\phi_{RP})), \qquad (8)$$

and

$$I_4 = I_0(1 + \gamma \cos(\phi + \phi_{BS} + \phi_{RP})). \qquad (9)$$

Using Eqs. (1) and (9), and Eqs. (2) and (8), resulted in

$$I_4 - I_1 = \gamma \sin\left(\phi + \frac{3}{2}\phi_{BS} + \frac{3}{2}\phi_{RP}\right)\sin\left(\frac{1}{2}\phi_{BS} + \frac{1}{2}\phi_{RP}\right), \qquad (10)$$

$$I_2 - I_3 = \gamma \sin\left(\phi + \frac{3}{2}\phi_{BS} + \frac{3}{2}\phi_{RP}\right)\sin\left(\frac{3}{2}\phi_{BS} + \frac{3}{2}\phi_{RP}\right). \qquad (11)$$

Using Eqs. (10) and (11), the phase difference ϕ can be expressed as

$$\phi = \tan^{-1}\left[\tan\left(\frac{A}{2}\right) \cdot \frac{(I_2 - I_3) + (I_4 - I_1)}{(I_4 + I_1) - (I_2 + I_3)}\right] - \frac{3}{2}A, \qquad (12)$$

where

$$A = 2\tan^{-1}\left[\frac{3(I_4 - I_1) - (I_2 - I_3)}{(I_2 - I_3) + (I_4 - I_1)}\right]^{1/2}. \qquad (13)$$

Therefore, according to Eqs. (12) and (13), when the phase difference is accurately measured, the refractive index of the tested specimen n_2 can be obtained using Eq. (7).

3. Experimental setup and results

To demonstrate the feasibility of the proposed method, various mixtures of the tested specimens were measured at room temperature of 25 °C, including air, glycerol, and castor oil with refractive indices of 1, 1.473, and 1.480, respectively, at a wavelength of 632.8 nm. An He-Ne laser with a wavelength of 632.8 nm was used as the light source. A high-resolution motorized rotation stage (Model SGSP-60-WPQ, Sigma Koki, Inc.) with an angular resolution of 0.005° was used to mount and rotate the tested apparatus. The tested apparatus consisted of a SF11 right-angle prism ($n_1 = 1.7780$) with a test box on its base. To achieve high sensitivity, the incident angle θ_1 of light at the base of the prism was set to 57°. Additionally, the beam splitting device consisted of three BK7 beamsplitters (10BC16NP.4, Newport) and two BK7 right-angle prisms (10BR08, Newport). The interferometric signals were captured using a CMOS camera (C) with an 8-bit gray level, and a personal computer and Matlab software were used to analyze the captured images. The experimental results are shown in Figs. 2–5 with samples of air and glycerol, and air, glycerol, and castor oil. Figs. 2 and 3 show four interferometric images of various phase distributions, and Figs. 4 and 5 show the refractive index distributions. The results in Figs. 4 and 5 show that the measured refractive
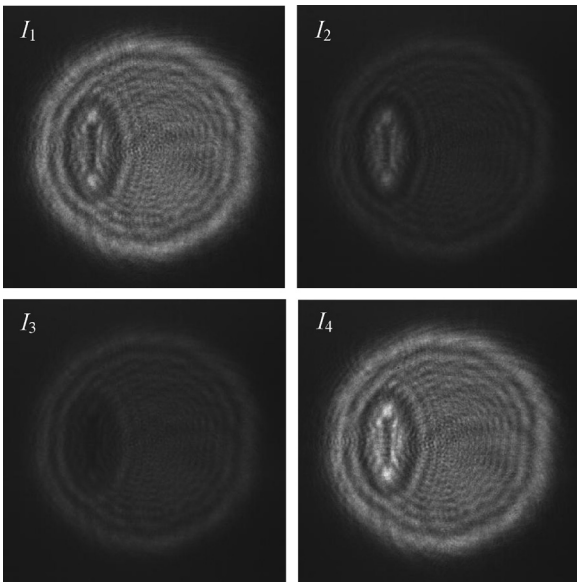
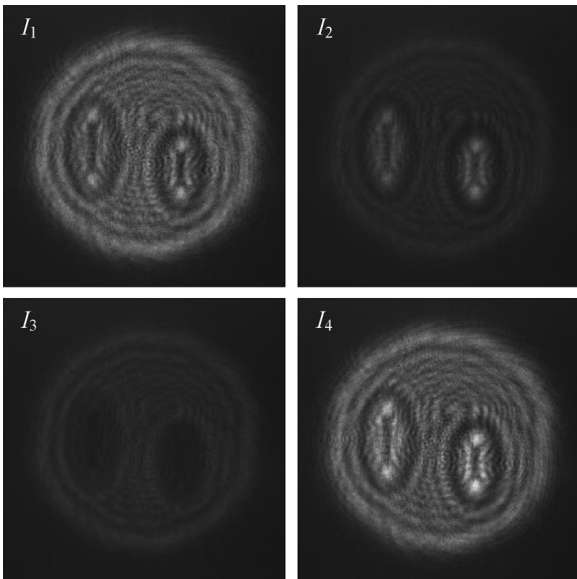**Fig. 2.** Four interferometric images of various phase distributions for samples of air and glycerol.

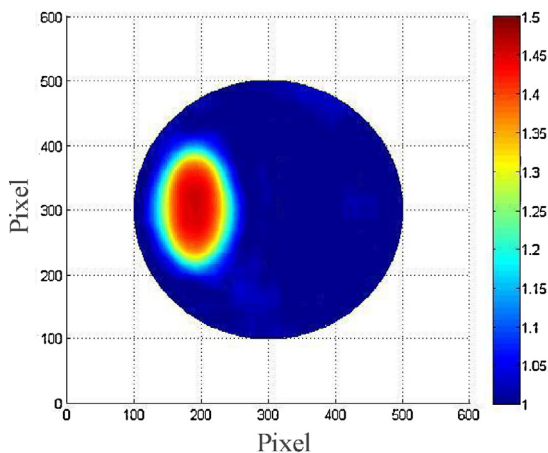**Fig. 3.** Four interferometric images of various phase distributions for samples of air, glycerol, and castor oil.

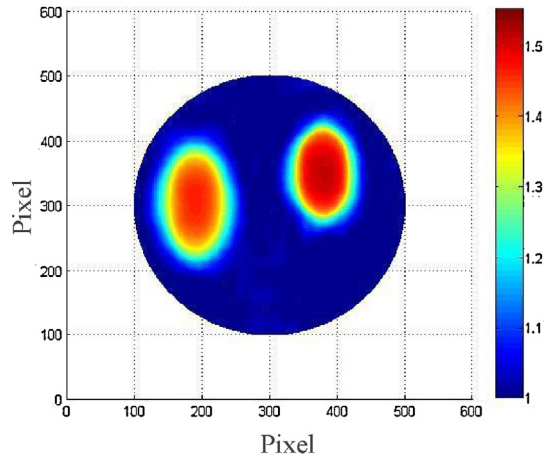**Fig. 4.** The refractive index distribution for samples of air and glycerol.

Fig. 5. The refractive index distribution for samples of air, glycerol, and castor oil.

indices of air, glycerol, and castor oil are 1.005, 1.468, and 1.493, respectively. The experimental data corresponded with the theoretical values.

4. Discussions

This method uses the phenomenon of total internal reflection; the phase difference between the *p*- and *s*-polarized light varied significantly with the refractive index of the tested specimens. This substantially increased the measurement sensitivity. Furthermore, Fig. 6 shows the relationship of the phase difference ϕ versus the incident angle θ_1 under the following conditions of the relative refractive indices: $n = 0.562$ (air), 0.828 (glycerol), and 0.832 (castor oil). Fig. 6 shows a larger phase difference variation between samples when the incident angle was set to the critical angle of the maximal relative refractive index. This can easily distinguish various tested samples and increase the measurement resolution. Therefore, the incident angle at the base of the prism in this experiment was set to $\theta_1 = 57°$.

To find the resolution, the differential deviation of Eq. (7) was calculated. Therefore, the error of the measured refractive index Δn_2 can be calculated as

$$\Delta n_2 \cong \left| \frac{\partial n_2}{\partial \phi} \right| \times \Delta \phi = \frac{\tan(\phi/2)\sec^2(\phi/2)\sin\theta_1\tan^2\theta_1}{2\sqrt{1 - \tan^2(\phi/2)\tan^2\theta_1}} \times \Delta\phi, \quad (14)$$

where $\Delta\phi$ denotes the error of the measured phase difference. Considering the error of CCD resolved phase and the polarization mixing error [12], the measurement error $\Delta\phi$ was calculated as
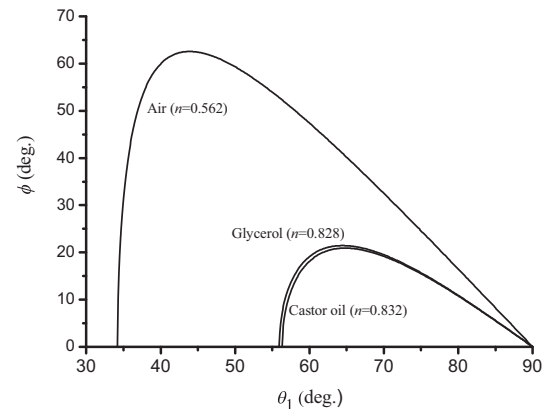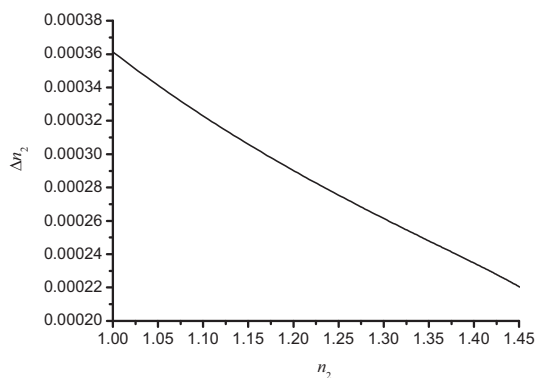

Fig. 6. The relationship of phase difference ϕ versus the incident angle θ_1 at the relative refractive index *n*.

Fig. 7. The relationship of the measurement resolution Δn_2 and the refractive index n_2.

$0.0141°$. By substituting the experimental conditions and results into (14), the relationship of the measurement resolution Δn_2 and the refractive index n_2 can be obtained, as shown in Fig. 7. The figure shows a higher resolution when n_2 is larger, and the measurement resolution can be higher than 3.65×10^{-4} RIU.

5. Conclusion

This paper proposes a technique of simultaneous phase-shift interferometry for measuring the full-field refractive index based on the phenomenon of total internal reflection and using a beam splitting device. Experiments involving various mixtures of air, glycerol, and castor oil confirmed the feasibility of this method. The measurement resolution can be higher than 3.65×10^{-4} RIU. This method offers the benefits of a simple structure, high stability, ease of operation, and real-time measurement.

References

[1] C. Huang, C. Chou, M. Chang, Direct measurement of refractive indices of a linear birefringent retardation plate, Opt. Commun. 133 (1997) 11–16.
[2] Y.S. Ghim, S.W. Kim, Thin-film thickness profile and its refractive index measurements by dispersive white-light interferometry, Opt. Express 14 (2006) 11885–11889.
[3] S.J. Chen, Y.D. Su, F.M. Hsiu, C.Y. Tsou, Y.K. Chen, Surface plasmon resonance phase-shift interferometry: real-time DNA microarray hybridization analysis, Proc. SPIE 18 (2003) 4966.
[4] C.L. Wong, H.P. Ho, Y.K. Suen, S.K. Kong, Q.L. Chen, W. Yuan, S.Y. Wu, Real-time protein biosensor arrays based on surface plasmon resonance differential phase imaging, Biosens. Bioelectron. 24 (2008) 606–612.
[5] J.G. Webster, The Measurement, Instrumentation and Sensors Handbook, CRC Press, Boca Raton, 1999, pp. 61-4–61-5.
[6] S.J. Chen, Y.D. Su, F.M. Hsiu, C.Y. Tsou, Y.K. Chen, Surface plasmon resonance phase-shift interferometry: real-time DNA microarray hybridization analysis, J. Biomed. Opt. 10 (3) (2005) 034005.
[7] C.L. Wong, H.P. Ho, T.T. Yu, Y.K. Suen, W.W. Chow, S.Y. Wu, W.C. Law, W. Yuan, W.J. Li, S.K. Kong, C. Lin, Two-dimensional biosensor arrays based on surface plasmon resonance phase imaging, Appl. Opt. 46 (2007) 2325–2332.
[8] Z.C. Jian, P.J. Hsieh, H.C. Hsieh, H.W. Chen, D.C. Su, A method for measuring two-dimensional refractive index distribution with the total internal reflection of p-polarized light and the phase-shifting interferometry, Opt. Commun. 268 (2006) 23–26.
[9] Y.D. Su, S.J. Chen, T.L. Yen, Common-path phase-shift interferometry surface plasmon resonance imaging system, Opt. Lett. 30 (12) (2005) 1488–1490.
[10] Y.D. Su, K.C. Chiu, N.S. Chang, H.L. Wu, S.J. Chen, Study of cell-biosubstrate contacts via surface plasmon polariton phase microscopy, Opt. Express 18 (2010) 20125–20135.
[11] J.Y. Lee, T.K. Chou, H.C. Shin, Polarization-interferometric surface-plasmon-resonance imaging system, Opt. Lett. 33 (5) (2008) 434–436.
[12] M.H. Chiu, J.Y. Lee, D.C. Su, Complex refractive-index measurement based on Fresnel's equations and uses of heterodyne interferometry, Appl. Opt. 38 (1999) 4047–4052.